Available online at www.sciencedirect.com
ScienceDirect
Journal of Power Sources 175 (2008) 800–805
JOURNAL OF POWER SOURCES
www.elsevier.com/locate/jpowsour

Short communication

Solid oxide fuel cells with bi-layered electrolyte structure

Xinge Zhang *, Mark Robertson, Cyrille Decès-Petit, Yongsong Xie, Rob Hui, Wei Qu, Olivera Kesler, Radenka Maric, Dave Ghosh

Institute for Fuel Cell Innovation, National Research Council Canada, 4250 Wesbrook Mall, Vancouver, B.C. V6T 1W5, Canada

Received 10 August 2007; received in revised form 2 October 2007; accepted 3 October 2007
Available online 13 October 2007

Abstract

In this work, we have developed solid oxide fuel cells with a bi-layered electrolyte of 2 μm SSZ and 4 μm SDC using tape casting, screen printing, and co-firing processes. The cell reached power densities of 0.54 W cm^{-2} at 650 °C and 0.85 W cm^{-2} at 700 °C, with open circuit voltage (OCV) values larger than 1.02 V. The electrical leaking between anode and cathode through an SDC electrolyte has been blocked in the bi-layered electrolyte structure. However, both the electrolyte resistance (R_{el}) and electrode polarization resistance ($R_{p,a+c}$) increased in comparison to cells with single-layered SDC electrolytes. The formation of a solid solution of (Ce, Zr)O_{2-x} during sintering process and the flaws in the bi-layered electrolyte structure seem to be the main causes for the increase in the R_{el} value (0.32 Ω cm^2) at 650 °C, which is almost one order of magnitude higher than the calculated value.

Keywords: SOFC; Low temperature; Bi-layer electrolyte; SDC; SSZ

1. Introduction

A high-operating temperature is one of the main barriers for a wide-scale adoption of solid oxide fuel cell (SOFC) technology [1]. Therefore, much work is focused on the development of reduced temperature SOFCs [2]. The practical operating temperature of an SOFC is mainly determined by the conductivity and thickness of the electrolyte. Samaria-doped ceria (SDC) is a promising material for the electrolyte in reduced temperature SOFCs [3,4]. SDC exhibits a relatively high conductivity of 0.1 S cm^{-1} at 800 °C [5], 2–3 times higher than that of yttria-stabilized zirconia (YSZ). Its thermal expansion coefficient (12.5×10^{-6} K^{-1}) is also more compatible with that of the Ni-cermet anode and commercial ferritic stainless steel interconnect, than that of YSZ. Although the material exhibits better chemical and structural compatibility with electrodes as well as higher ionic conductivity than YSZ, the reduction of Ce^{4+} to Ce^{3+} induces n-type electronic conduction, which tends to decrease the power output of solid oxide fuel cells due to an internal electrical shorting. The problem can be partially solved by decreasing the operating temperature to below 600 °C, as the SDC electrolyte domain is expanded at lower temperatures [6]. However, even at 600 °C, the cell appears intolerant to internal shorting due to the low electrical resistance of the thin electrolyte [7]. It has been reported that this problem can be eliminated by using a barrier of thin ZrO_2-based electrolyte layer deposited on the anode side of the SDC layer to improve the stability of the SDC electrolyte layer under the reducing atmosphere. This configuration is generally called a bi-layered electrolyte structure [8–11]. The ionic conductivity of scandia-stabilized zirconia (SSZ) is the highest among all the ZrO_2-based electrolytes [12]; however, it is not considered as a candidate electrolyte for reduced temperature SOFCs since its conductivity decreases rapidly with temperatures below 800 °C [13]. When a bi-layer SDC/SSZ electrolyte is used, the SSZ layer acts mainly as the barrier. If the SSZ layer thickness is in the range of a few micrometers to a few hundred nanometers, its relatively low conductivity will not contribute significantly to the overall ohmic loss of the bi-layer SDC/SSZ electrolyte for SOFCs. For the fabrication of anode-supported SOFCs, wet ceramic processes like screen printing and tape casting have been widely adopted, and have proven to be scalable and cost-effective [14]. A peak power

* Corresponding author. Tel.: +1 604 221 3077; fax: +1 604 221 3001.
E-mail address: xinge.zhang@nrc.gc.ca (X. Zhang).

0378-7753/$ – see front matter.
doi:10.1016/j.jpowsour.2007.10.021

density of 0.6 W cm^{-2} at 700 °C has previously been obtained in an anode-supported cell with a YSZ/SDC bi-layered electrolyte by electrophoretic deposition [15] and screen printing and co-firing [9]. Recently, Wang et al. [16] used a multi-layer tape casting procedure to fabricate an anode-supported 5 μm SSZ/10 μm GDC bi-layered electrolyte cell. With an LSCF-GDC composite cathode sintered at 1100 °C, they obtained a maximum power density of 0.63 W cm^{-2} and an area-specific resistance (ASR) of 0.99 Ω cm^2 at 850 °C in the single cell with H_2/O_2 as the operating gases.

In this work, anode-supported cells with SSZ/SDC bi-layered electrolytes were fabricated by screen printing and co-firing under optimized processing conditions to control the layer thickness. The obtained cell results show promising for reduced temperature applications.

2. Experimental

2.1. Starting materials and cell architectures

Table 1 lists the starting ceramic powder materials used in this study. All the materials for cell fabrication were commercially obtained. Table 2 lists the cell materials, thicknesses, and processing conditions. The cell structure consists of a NiO–YSZ cermet substrate, NiO–SSZ anode layer, SSZ/SDC bi-layered electrolyte, and SSC cathode. 1 at.% Co was added to the SDC powder for controlling the sintering behaviour—the treatment and sinterability improvements have been reported in our previous work [17]. A 57 wt% NiO and 43 wt% YSZ powder mixture was used for the NiO–YSZ cermet substrate. The composition of the NiO–SSZ anode was 56 wt% NiO and 44 wt% SSZ. The cell was fabricated by tape casting the substrate, screen printing the anode and the electrolyte on the substrate tape, and then co-firing at 1400 °C for 2 h, followed by cathode printing and sintering in situ during the test. Further details about the cell fabrication process and characterization can be found in [4,7,10]. The cell used in this study was 16 mm in diameter. The printed $Sm_{0.5}Sr_{0.5}CoO_3$ (SSC) cathode area was 0.50 cm^2, which was the cell's effective area used in this work.

The average density of the cell substrate after the anode layer deposition was 5.1 g cm^{-3} measured by Archimedes' method. It indicated a 19.4% porosity in the NiO–YSZ cermet substrate based on the cermet substrate composition of 57 wt% NiO. The substrate porosity will increase to approximately 37% after reducing NiO to Ni with the hydrogen gas.

2.2. Cell electrochemical and morphological characterizations

The cell electrochemical measurement was conducted in a lab-built horizontal button cell test station, which has been described before [4,7,9]. The cell was heated up to 650 °C at a ramp rate of 300 °C h^{-1}, and held at 650 °C for 1 h for reduction and in situ sintering of the cathode layer. The reduction was carried out by anode gas with H_2 concentrations varying step-wise from 10%, 20%, 40%, 60%, to a final 100%, with N_2 balance. Each concentration (balanced by N_2) was held for 15 min. The anode gas was first passed at a flow rate of 100 ml min^{-1} through a bubbler-type humidifier at room temperature. The humidified hydrogen gas (corresponding to 3% H_2O content) was then introduced to the anode side during the cell test. Ambient air was introduced at a flow rate of 100 ml min^{-1} to the cathode side. Electrochemical measurements were performed at temperatures ranging from 550 °C to 800 °C. The *I–V* curve and impedance tests were performed at intervals of 50 °C between 550 °C and 800 °C. Cell performance was measured with a Multi-channel Potentiostat/Galvanostat (Solartron 1480 8-channel multi-stat) coupled with a 1260 FRA using the software Corr-Ware and Z-Plot. The current–voltage–power (*I–V–*P) curves were obtained using linear sweep voltametry at a sweep rate of 4 mV s^{-1} from OCV to 0.3 V. The impedances were measured in the frequency

Table 1
Chemical composition, properties, and suppliers of starting materials

Material for	Composition	Properties	Supplier
Cathode	$Sm_{0.5}Sr_{0.5}CoO_3$ (SSC)	D50: 0.80 μm, surface area: 5.16 m^2 g^{-1}	Praxair
Electrolyte	$(SmO_{1.5})_{0.2}(CeO_2)_{0.8}$ (SDC)	D50: 0.40 μm, surface area: 7.08 m^2 g^{-1}	Praxair
	$Sc_{0.2}Ce_{0.01}Zr_{0.79}O_{2-x}$ (SSZ)	D50: 0.43 μm, surface area: 12.3 m^2 g^{-1}	Daiichi Kigenso Kagaku Kogyo
	$Co(NO_3)_3$ $6H_2O$	Sintering aid for SDC–1%Co	Alfa Aesar
Anode	NiO (type F)	D50: 1.0 μm, surface area: 4.0 m^2 g^{-1}	Novamet
Cermet substrate	NiO (standard)	D50: 16.0 μm, surface area: <1 m^2 g^{-1}	
	8YSZ (YSZ)	D50: 0.520 μm, surface area: 6.2 m^2 g^{-1}	Tosoh

Table 2
Cell materials, thicknesses, and processing conditions

Cell component	Material	Thickness (μm)	Process	Firing condition		Porosity
Cathode	SSC	50	Stencil printing	In situ up to 800 °C		∼40%
Electrolyte	SDC–1%Co	4	Screen printing	1400 °C	2 h	Dense and pass Helium cross-leak test [7,9]
	SSZ	2				
Anode	NiO–SSZ	10	Screen printing			19% before reduction, 37% after reduction
Substrate	NiO–YSZ	800	Tape casting			

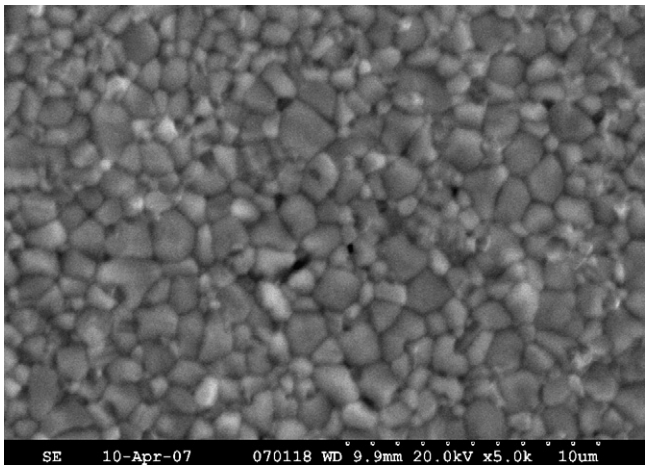

Fig. 1. SEM image of the bi-layered SDC/SSZ electrolyte surface.

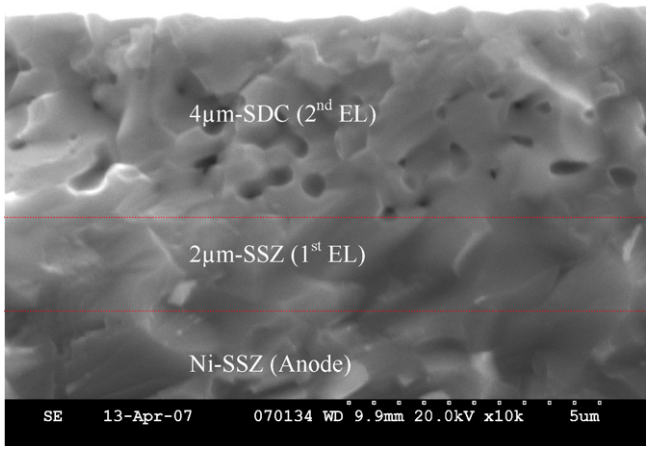

Fig. 2. SEM image of cross-sectional view of the bi-layered SDC/SSZ electrolyte.

range of 10 kHz–0.1 Hz with a perturbation potential amplitude of 50 mV.

The morphologies of the tested cells were observed using a scanning electron microscope (SEM, Hitachi S-3500N), coupled with energy dispersive spectrometry (EDS) and X-ray diffraction techniques for elemental and phase analysis, respectively. Each sample was coated with Au–Pd alloy before observation.

3. Results and discussion

3.1. Electrolyte thickness control

In order to effectively utilize the SSZ/SDC bi-layer electrolyte concept for reduced temperature SOFCs, the SSZ layer should be as thin as possible and also be gas impermeable. We examined the paste solid loading and screen mesh effects on the SSZ layer thickness. It was found that by reducing the solid loading to 7.5 vol.% and increasing the screen mesh number from 200# to 325#, the final printed layer thickness per print-pass after firing could be controlled to under 2 μm. It was also noticed that the thickness of the anode layer played an important role in the final electrolyte quality during the co-firing at 1400 °C for 2 h. All the cells with bi-layered electrolytes and anode layer passed the 1 psi Helium cross-leakage test, indicating the intactness and density of the electrolyte layer, as illustrated in Figs. 1 and 2.

The interdiffusion (or interaction) between electrolyte layers at co-firing conditions is the main concern, which has been reported by [15,16,19]. Fig. 3 shows the EDS elemental mapping at the cross-section of the electrolyte portion of a cell. The results clearly indicate that the different layers of the anode, SSZ, and SDC can be easily identified. The interdiffusion (or interaction) zone, if it is generated during the co-firing, seems to be within 1 μm; otherwise, we would not have been able to clearly see the SSZ layer, which is designed and observed to have a thickness of 2 μm.

It is worthwhile to mention that SDC–1%Co does not show any sinterability improvement in comparison to pure SDC [9]. In our previous work with bulk pellets, it showed about a 200–300 °C difference in the temperature required for full densification [17], and many authors reported similar results. Our explanation is that the Co-sintering aid could not take effect in this work due to vaporization loss of the Co at high temperature, and consequent limited liquid phase formation in the small electrolyte thickness.

3.2. Cell test result

An SSC cathode was applied onto the surface of the bi-layered electrolyte by stencil printing followed by drying and in situ sintering at 650 °C. The unit cell thus prepared was characterized for its electrochemical performance. Fig. 4 shows the cell performance with the SSC cathode in situ sintered. It can be seen that the cell shows very high performance in the tested temperature range of 550–800 °C. The peak power density reached 1.8 W cm^{-2} at 800 °C, and approximately 0.54 W cm^{-2} even at 650 °C. What is most significant is that the cell showed a very high OCV value, 1.03 V, in comparison to the single-layer 20 μm-SDC electrolyte cell, which only showed 0.84 V at 650 °C [17]. A high OCV value indicates that there is very low electronic conductivity and few physical defects (cracks, pin-holes, etc.) in the SSZ/SDC bi-layered electrolyte. Compared to the results in previously reported literature [9,15,16], our bi-layered cells fabricated by conventional ceramic processing showed an improved performance, and exhibit significant power density even at 650 °C.

Fig. 5 shows the electrochemical impedance spectra of the cell at different temperatures. The measured results are also listed in Table 3. In comparison with our previous work on cells with thin SDC electrolytes (10 μm) [7], it is very clear that the values of electrolyte resistance, R_{el}, and electrode polarization resistances, $R_{p,a+c}$, have increased significantly along with the increase in the OCV values. The reported R_{el} and $R_{p,a+c}$ values of the cell with 10 μm SDC electrolyte are only 0.10 Ω cm^2 and 0.13 Ω cm^2 at 600 °C, respectively, while for the bi-layered electrolyte in this study they increased to 0.46 Ω cm^2 and 0.70 Ω cm^2, respectively. The increase in $R_{p,a+c}$ may have had contributions from the electrodes since the compositions in

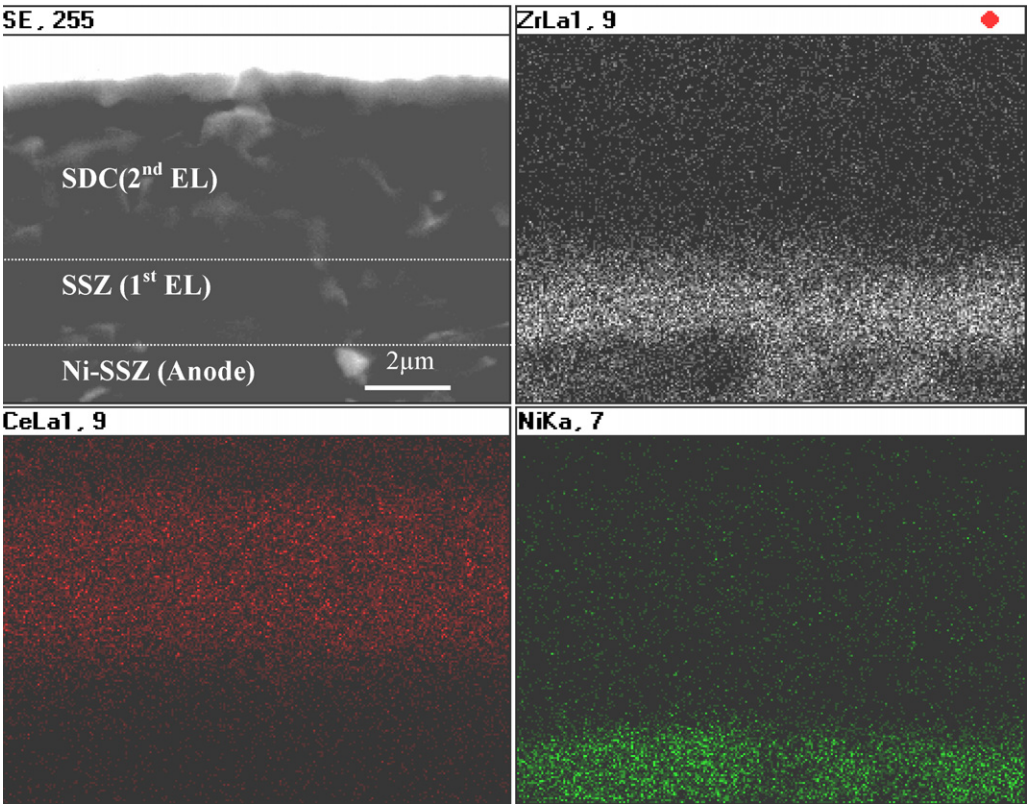

Fig. 3. EDS elemental mapping at the cross-sectional view of the bi-layered electrolyte cell before applying cathode.

these two studies are different. In the case of the cell with SDC electrolyte, a Ni–SDC anode was used, while in this study of bi-layered electrolytes, however, the anode is Ni–SSZ. Since SDC has higher ionic and electronic conductivities than those of SSZ, the SDC mixed conductor in the anode will help to improve the anode performance. The previous study also used a composite SSC–SDC cathode, while this study uses a single phase SSC cathode. In addition, mixed conductivity in the electrolyte can make the apparent polarization resistance of the electrodes smaller than their actual values due to the electronic current that pass through the electrolyte. Furthermore, an increment in R_{el} is obviously noticeable. In this study, R_{el} consisted of three parts: $R_{el,SSZ}$, $R_{el,SDC}$, and $R_{interface}$. Based on the SSZ ionic conductivity of 0.08 S cm^{-1} at 800 °C [19], the $R_{el,SSZ}$ of the 2 μm thick SSZ electrolyte was approximately 0.0025 Ω cm^2. Meanwhile,

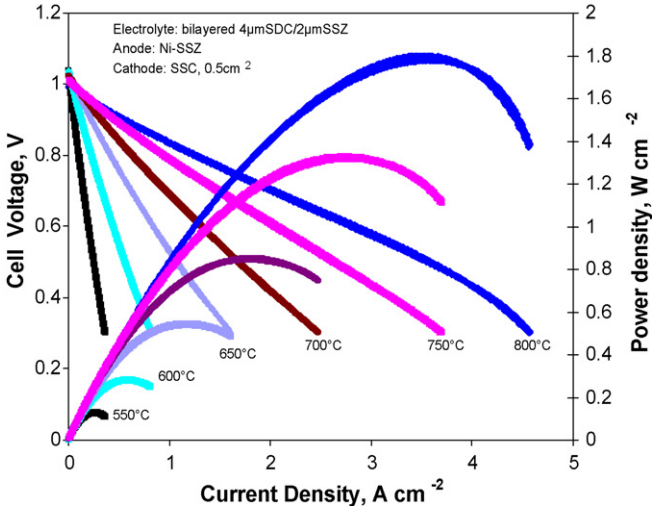

Fig. 4. Current–voltage–power curves of the bi-layer electrolyte cell at different operating temperatures.

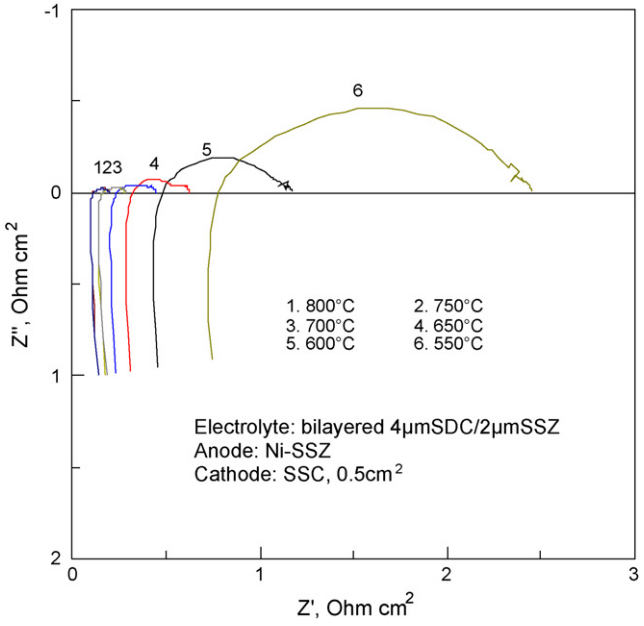

Fig. 5. EIS spectra of the cell at different temperatures.

Table 3
Cell performance and cell resistances

Temperature (°C)	OCV (V)	MPD (W cm^{-2})	R_{el} (Ω cm^2)	$R_{p,a+c}$ (Ω cm^2)	R_{cell} (Ω cm^2)
550	1.037	0.127	0.760	1.717	2.477
600	1.038	0.281	0.461	0.704	1.165
650	1.025	0.545	0.311	0.390	0.701
700	1.023	0.850	0.222	0.211	0.433
750	1.009	1.326	0.152	0.127	0.278
800	0.994	1.800	0.105	0.091	0.196

OCV: open circuit voltage, MPD: maximum power density, R_{el}: SSZ/SDC bi-layered electrolyte ohmic resistance from EIS, $R_{p,a+c}$: electrode polarization resistance from EIS, R_{cell}: cell resistance from EIS ($R_{cell} = R_{el} + R_{p,a+c}$).

Table 4
Ionic conductivity (σ_i) and electronic conductivity (σ_e) of YSZ, GDC and the mixed composites at 800 °C [20]

Material	Nominal composition	σ_i (S m^{-1})	σ_e (S m^{-1})
YSZ	$Zr_{0.85}Y_{0.15}O_{1.93}$	5.4	7.29×10^{-11}
GDC	$Ce_{0.80}Gd_{0.20}O_{1.90}$	8.7	8.18×10^{-4}
Reaction product	$Ce_{0.37}Zr_{0.38}$ $Gd_{0.18}Y_{0.07}O_{1.87}$	0.125	3.99×10^{-4}
Interlayer	$Ce_{0.43}Zr_{0.43}$ $Gd_{0.10}Y_{0.04}O_{1.93}$	0.603	3.88×10^{-4}

the $R_{el,SDC}$ of the 4 μm thick SDC electrolyte was estimated to be 0.0032 Ω cm^2, according to our measured results and published conductivity data of SDC of 0.12 S cm^{-1} at 800 °C [5,6]. In comparison with the R_{el} value (0.105 Ω cm^2) at 800 °C shown in Table 3, both contributions can be considered negligible. Thus, the $R_{interface}$ can be as high as 0.099 Ω cm^2, over 90% of the total electrolyte ohmic resistance. It is well reported that the interdiffusion produced by the (Zr,Ce)O_2-based solid solution, the conductivity of which is 2–4 times lower than that of the SSZ, is one to two orders of magnitude lower than that of the SDC [18]. Table 4 lists the ionic conductivity and electronic conductivity of YSZ, GDC, and the mixed composites at 800 °C [20]. It is well known that the interaction produces a poor ionic conducting phase. This gives an explanation as to why such a thin layer (even less than 1 μm) dominates the R_{el} value in the bi-layered electrolyte. The thickness of the (Zr,Ce)O_2-based solid solution formed at the SSZ/CGO interface during high temperature sintering plays a key role in the R_{el} value. The $R_{interface}$ in this study is almost 3 times lower than the reported value of 0.283 Ω cm^2 for the SSZ/GDC system, which showed an interdiffusion layer zone of about 3 μm in thickness by EDS mapping [16]. The thickness of the interdiffusion layer zone is obviously related to the starting material and processing conditions. We used an SSZ/SDC electrolyte combination and fired at 1400 °C for 2 h, while Wang et al. [16] used SSZ/GDC fired at the same sintering temperature, but for 4 h. Since interdiffusion is a thermally activated process, reducing sintering temperature and sintering time should be an effective approach to reducing the $R_{interface}$. However, we found that when decreasing the sintering temperature to 1300 °C, the bi-layered electrolyte is not well bonded together, and also the electrolyte, especially the SDC layer, is not well sintered. As a result, there is no improvement in the cell quality or cell performance.

We calculated the apparent activation energy for the total electrical conduction of the bi-layered electrolyte based on the values listed in Table 3 and found that the apparent activation energy is 64.77 kJ mol^{-1}, which is slightly higher than, but very close to, what we obtained before for a single-layered SDC electrolyte (61.89 kJ mol^{-1} [7]) and other published values of 61.75 kJ mol^{-1} [6] and 59.2 kJ mol^{-1} [21]. This reveals that the conduction mechanism of the bi-layered electrolyte had not changed significantly from the main electrolyte of SDC in this study.

The results obtained in this study illustrate that the fabrication of anode-supported electrolyte films for planar SOFCs with an SSZ electrolyte electron-blocking layer is possible by multi-layer screen printing on tape-cast substrates. The technique is both cost-effective and feasible. The interfacial reaction between SSZ and SDC can be tailored to some extent to reach a higher cell performance. Future work will focus on cell stability and further cell performance improvement.

4. Conclusion

Cermet-supported solid oxide fuel cells with bi-layered electrolytes of SSZ and SDC were successfully prepared by multi-layer screen printing on tape-cast NiO–YSZ cermet substrates. No cracking or delaminating was observed after co-firing at 1400 °C for 2 h. The open circuit voltage of the cell reached over 1.02 V below 750 °C, and the maximum power density reached 1.8 W cm^{-2} at 800 °C. The internal shorting of a single-layer SDC electrolyte cell has been mostly eliminated. Electrochemical impedance measurement results revealed that the ohmic resistance at the SSZ/SDC interface ($R_{interface}$) dominates the whole electrolyte resistance. Meanwhile, the electrode polarization resistance ($R_{p,a+c}$) is approximately half of the total cell resistance over the temperature range from 650 °C to 800 °C. This work demonstrates that cost-effective wet ceramic processing can be useful for bi-layered electrolyte cell fabrication. The demonstrated cell performance is very attractive for SOFC applications.

Acknowledgement

The authors would like to thank the National Research Council of Canada for supporting the low temperature SOFC project.

References

[1] S.P.S. Badwal, K. Foger, Ceram. Int. 22 (1996) 257.
[2] W.S. Jang, S.H. Hyun, S.G. Kim, J. Mater. Sci. 37 (2002) 2535.
[3] Z. Shao, S.M. Haile, Nature 431 (2004) 170.
[4] X. Zhang, M. Robertson, S. Yick, C. ces-Petit, E. Styles, W. Qu, Y. Xie, R. Hui, J. Roller, O. Kesler, R. Maric, D. Ghosh, J. Power Sources 160 (2006) 1211.
[5] T. Shimonosono, Y. Hirata, Y. Ehira, S. Sameshima, T. Horita, H. Yokokawa, Solid State Ionics 174 (2004) 27.
[6] V.V. Kharton, F.M. Figueiredo, L. Navarro, E.N. Naumovich, A.V. Kovalevsky, A.A. Yaremchenko, A.P. Viskup, A. Carneiro, M.B. Marques, J.R. Frade, J. Mater. Sci. 36 (2001) 1105.
[7] X. Zhang, M. Robertson, C. ces-Petit, W. Qu, O. Kesler, R. Maric, D. Ghosh, J. Power Sources 164 (2007) 668.
[8] T. Tsai, E. Perry, S. Barnett, J. Electrochem. Soc. 144 (1997) L130–L132.
[9] X. Zhang, M. Robertson, C. ces-Petit, Y. Xie, R. Hui, S. Yick, E. Styles, J. Roller, O. Kesler, R. Maric, D. Ghosh, J. Power Sources 161 (2006) 301.
[10] D. Yang, X. Zhang, S. Nikumb, C. ces-Petit, R. Hui, R. Maric, D. Ghosh, J. Power Sources 164 (2007) 182.
[11] C. Brahim, A. Ringuede, E. Gourba, M. Cassir, A. Billard, P. Briois, J. Power Sources 156 (2006) 45.
[12] Y. Arachi, H. Sakai, O. Yamamoto, Y. Takeda, N. Imanishai, Solid State Ionics 121 (1999) 133.
[13] T. Ishii, T. Iwata, Y. Tajima, A. Yamaji, Solid State Ionics 57 (1992) 153.
[14] Y. Lin, S.A. Barnett, Electrochem. Solid -State Lett. 9 (2006) A285–A288.
[15] M. Matsuda, T. Hosomi, K. Murata, T. Fukui, M. Miyake, J. Power Sources 165 (2007) 102.
[16] Z. Wang, J. Qian, J. Cao, S. Wang, T. Wen, J. Alloys Compd. 437 (2007) 264.
[17] X. Zhang, C. ces-Petit, S. Yick, M. Robertson, O. Kesler, R. Maric, D. Ghosh, J. Power Sources 162 (2006) 480.
[18] M. Price, J. Dong, X. Gu, S.A. Speakman, E.A. Payzant, T.M. Nenoff, J. Am. Ceram. Soc. 88 (2005) 1812.
[19] D.S. Lee, W.S. Kim, S.H. Choi, J. Kim, H.W. Lee, J.H. Lee, Solid State Ionics 176 (2005) 33.
[20] A. Tsoga, A. Naoumidis, D. Stover, Solid State Ionics 135 (2000) 403.
[21] H. Inaba, H. Tagawa, Solid State Ionics 83 (1996) 1.